



## Hyaluronic acid based hydrogels attenuate inflammatory receptors and neurotrophins in interleukin-1 beta induced inflammation model of nucleus pulposus cells

Title	Hyaluronic acid based hydrogels attenuate inflammatory receptors and neurotrophins in interleukin-1 beta induced inflammation model of nucleus pulposus cells
Author(s)	Isa, Isma Liza Mohd;Srivastava, Akshay;Tiernan, David;Owens, Peter;Rooney, Peadar;Dockery, Peter;Pandit, Abhay
Publication Date	2015-04-14
Publisher	American Chemical Society
Repository DOI	<a href="https://doi.org/10.1021/acs.biomac.5b00168">10.1021/acs.biomac.5b00168</a>

# HYALURONIC ACID BASED HYDROGELS ATTENUATE INFLAMMATORY RECEPTORS AND NEUROTROPHINS IN INTERLEUKIN-1 $\beta$ INDUCED INFLAMMATION MODEL OF NUCLEUS PULPOSUS CELLS

*Isma Liza Mohd Isa,<sup>†</sup> Akshay Srivastava,<sup>†</sup> David Tiernan,<sup>†</sup> Peter Owens,<sup>‡</sup> Peadar Rooney,<sup>†</sup> Peter Dockery,<sup>‡</sup> and Abhay Pandit\*,<sup>†</sup>*

<sup>†</sup>Centre for Research in Medical Devices (CÚRAM) and <sup>‡</sup>Centre for Microscopy and Imaging, National University of Ireland, Galway, Ireland

## ABSTRACT

Inflammation plays an important role in symptomatic intervertebral disc degeneration and is associated with the production of neurotrophins in sensitizing innervation into the disc. The use of high molecular weight (HMw) hyaluronic acid (HA) hydrogels offers a potential therapeutic biomaterial for nucleus pulposus (NP) regeneration as it exerts an anti-inflammatory effect and

provides a microenvironment that is more suitable for NP. Therefore, it was hypothesized that crosslinked HMw HA hydrogels modulate the inflammatory receptor of IL-1R1, MyD88 and neurotrophin expression of nerve growth factor (NGF) and brain-derived neurotrophic factor (BDNF) in an *in vitro* inflammation model of NP. The crosslinking system was optimized using various concentrations of 4-arm PEG-amine by determination of free carboxyl groups of HA, unreacted free amine groups of PEG-amine and surface morphology. The optimally crosslinked HA hydrogels were characterised for hydrolytic stability, enzymatic degradation and cytotoxicity on NP cells. The therapeutic effect of optimally crosslinked HA hydrogels was further investigated in IL-1 $\beta$  induced inflammation on NP cell cultures and the mechanism of HA in response to inflammation by examining the binding cell surface receptor of CD44. Hydrogel was optimally crosslinked at 75 mM PEG, stable in phosphate buffered saline, and showed greater than 40% resistance to enzymatic degradation. No cytotoxic effect of NP cells was observed after treatment with HA hydrogels for 1, 3 and 7 days. IL-1R1 and MyD88 receptors were significantly suppressed. Additionally, NGF and BDNF mRNA were down-regulated after treatment with crosslinked HA hydrogel. Possible protective mechanism of HA is shown by binding of CD44 receptor of NP cells to HA and prevent NP cells from further undergoing inflammation. These results indicate that optimally stabilized crosslinked HMw HA hydrogel has a therapeutic effect in response to inflammation-associated pain and becomes an ideal matrices hydrogel for NP regeneration.

## KEYWORDS

Intervertebral disc, inflammation, pain, hyaluronic acid, hydrogel.

## Introduction

Low back pain (LBP) is a common health problem that affects 60–80% of the population of developed countries at some stage in their lives.<sup>1,2</sup> Most patients recover from acute back pain within a month while some patients develop chronic back pain followed by long-term disability leading to morbidity and this causes severe socio-economic impact on the society.<sup>3,4</sup> The majority of cases of LBP are caused by intervertebral disc (IVD) degeneration,<sup>3,5</sup> and most patients remain asymptomatic with some experiencing discogenic pain.<sup>6</sup> Current therapy for IVD degeneration includes rehabilitation<sup>7</sup> and medication such as non-steroidal anti-inflammatory drugs (NSAIDs)<sup>8</sup> and systemic corticosteroids.<sup>7</sup> Surgical options include discectomy, spinal fusion and disc decompression, which are a last resort of treatment and may contribute to complications such as degeneration of the adjacent disc segment.<sup>9</sup>

The inflammatory process determines the severity and pain development of IVD degeneration.<sup>6,10</sup> Interleukin (IL)-1 is one of the most prominent pro-inflammatory cytokine expressed in IVD.<sup>6,11,12</sup> The study, by Le Maitre *et al.*, demonstrated that IL-1 $\beta$  and its receptor, IL-1R1, are increased by severity of degeneration in human disc samples and proposed that IL-1 $\beta$  is synthesized by native IVD cells.<sup>13</sup> Pro-inflammatory cytokines also correlate with the presence of neurotrophins and hyper-innervation in the IVD, and thereby develop pain.<sup>14</sup> A recent study illustrates that IL-1 $\beta$  induces mRNA expression of neurotrophins' nerve growth factor (NGF) and brain-derived neurotrophic factor (BDNF) in NP cells extracted from degenerated human IVD.<sup>15</sup> Hence, both NGF and BDNF indicate correlation with innervations in IVD via staining for an axonal growth marker such as protein gene product (PGP) 9.5 and GAP43.<sup>16,17,18</sup> Therefore, these inflammatory and neurotrophic factors are considered pathologic pathways of discogenic pain.

The neurotrophins' NGF and BDNF are neuronal survival and growth factors that support neuronal development, function and nociception and have been shown to induce nerve ingrowth into the IVD.<sup>19</sup> Studies demonstrate that NGF stimulates nerve ingrowth into the disc from the painful degenerated human disc<sup>20</sup> by promoting collateral sprouting of nociceptive nerve fibres<sup>21</sup> and modulating its function so as to generate pain.<sup>22</sup> Hence, neurons innervating the IVD are NGF sensitive by showing higher distribution of neurotransmitter calcitonin gene-related peptide (CGRP) in the dorsal root ganglion (DRG) neurons.<sup>18</sup> The nociceptive DRG neurons are categorized as NGF-sensitive neuron which conduct the pain information from peripheral region to the brain.<sup>23</sup> Whereas, BDNF regulates differentiation and survival of sensory neuron, and inflammatory pain hypersensitivity.<sup>24,25,26</sup> As a pain modulator, BDNF exerts fast excitatory (glutamatergic) and inhibitory (GABAergic/glycinergic) signals, and in contrast slow the peptidergic neurotransmission in spinal cord. Therefore, BDNF plays a role at the synapse in pain pathways at the central nervous system.<sup>27</sup> Gruber *et. al* found BDNF in culture degenerated human and rat disc samples, also triggers innervation and correlates with the severity of disc degeneration.<sup>28</sup>

Therefore, there is a compelling need to develop a therapy for painful IVD degeneration since the current treatment relieves the symptoms but does not treat the underlying degeneration. A tissue engineering approach targeting the multiple disrupted pathways underlying the cause of the disease is potentially a therapeutic strategy. A study from Andre *et al.* demonstrate a reduction of hyperalgesia in an inflammatory pain NP model of rat after treatment with antibodies specific to IL-1 $\beta$  and TNF- $\alpha$ .<sup>29</sup> Apart from that, the use of stem cells with or without scaffold using biodegradable biomaterials are also shown promising results in IVD regeneration.<sup>30</sup> In addition, designing a biomaterial platform in tissue engineering therapy

overcomes the limitation of short-term efficacy and delivery system of the intervention. The injectable crosslinked polyethylene glycol (PEG) and hyaluronic acid (HA) hydrogel incorporating mesenchymal precursor cells (MPCs) maintained cell viability and formed a chondrocyte-like tissue in IVD degeneration.<sup>31</sup> Thus, Daisuke *et al.* report human mesenchymal stem cells (MSCs) embedded in atelocollagen increased the disc height, preserved the NP tissue and restored the proteoglycan content in an *in vivo* model of IVD degeneration.<sup>32</sup> These results are supported by Marianna *et. al* show that thermoreversible HA-based hydrogel promoted the differentiation of human mesenchymal stem cells (MSCs) toward IVD-like phenotype.<sup>33</sup> Our previous work demonstrated that NP cells seeded in crosslinked PEG and collagen type II enriched with HA maintained the NP cell viability and up-regulated mRNA of type II collagen for matrix synthesis.<sup>34</sup> Recently, we prove that ADSC seeded in three dimensional (3D) type II collagen/HA microgels enhanced cell production and mimicked the NP-like phenotype.<sup>35</sup> In extension, we proposed to investigate the therapeutic effect of acellular HA hydrogels in inflammation milieu.

HA is a type of non-sulphate GAG composed of repeating units of glucuronic acid and N-acetyl-D-glucosamine connected through  $\beta$ -linkages.<sup>36</sup> At cellular level, HA is synthesized in a cytoplasmic surface of plasma membrane by HA synthases (HAS)<sup>37</sup> and is transported out from cells to pericellular space through a multidrug resistant transporter.<sup>38</sup> In NP tissue, HA is the backbone of proteoglycan aggregates that hold aggrecan molecules which are attached with highly anionic sulphated GAG.<sup>39</sup> The use of high molecular weight (HMw) HA ( $>1.0 \times 10^6$  Da) in osteoarthritis patients has been demonstrated to reduce inflammation and pain.<sup>40</sup> HA has also been associated with tissue repair by stimulating matrix synthesis of collagen type II in NP cells and chondrocytes,<sup>34,41</sup> modulating cellular function such as migration of aortic smooth muscle

cells<sup>42</sup> and maintenance of NP cells' phenotype.<sup>34,43</sup> However, the mechanism of HA in modulating cellular functions in disease systems remains unclear. The binding of the specific cell surface receptor of CD44 with HA has been implicated in cellular signaling and subsequently in regulating multiple cellular functions.<sup>44</sup> It has been previously shown that chondrocytes adhere to HA through binding to CD44 and thus induce cell proliferation and matrix synthesis.<sup>45</sup> Furthermore, the HA network in normal ECM promote clustering of the CD44 receptor to protect cells in response to the inflammation.<sup>46</sup> Nevertheless, none have been reported in NP tissue so far. The binding of CD44 and HA may play a key role in the mechanism of HA either in normal or in pathologic condition.

This biomaterial approach is based on supplementing inflamed NP cells with crosslinked HMw HA hydrogels. It was hypothesized that crosslinked HMw HA hydrogels alter the inflammatory receptor and neurotrophins expression in an IL-1 $\beta$  induced inflammation model of NP cells. To test this hypothesis specifically, a crosslinked HMw HA hydrogel system was developed by optimizing the crosslinking system and characterizing the optimal crosslinked hydrogels in a study of cytotoxicity and *in vitro* degradation. The therapeutic effect of crosslinked HMw HA hydrogels in inflamed NP cells was investigated by evaluating expression of inflammatory receptors of IL-1R1 and MyD88, neurotrophins' mRNA expression of NGF and BDNF, and the mechanism of action of HA through binding of cell surface receptor of CD44.

## **Experimental Section**

### **Materials and reagents**

HMw sodium hyaluronate ( $1.19 \times 10^6$  Da) was purchased from Lifecore Biomedical, USA. 4-arm PEG-amine Mw 2000 Da was purchased from JenKem Technology, USA Teflon™ tape was

purchased from Fisher Scientific, Ireland. Live/Dead® staining kit, alamarBlue® assay, Alexa Flour 488, Alexa Flour 564 and rhodamine phalloidin were purchased from Life Technologies, Ireland. Human recombinant IL-1 $\beta$  cytokine was purchased from PeproTech, USA. Anti-IL-1R1 antibody was purchased from Novus Biologicals, USA. Anti-MyD88 antibody and anti-CD44 antibody conjugated FITC were purchased from Abcam, Ireland. miRNeasy mini kit was purchased from Qiagen (Germany). TNBSA (2,4,6-trinitrobenzene sulfonic acid) was purchased from Thermo Scientific, USA. All other materials and reagents were purchased from Sigma Aldrich (Ireland) unless otherwise stated.

### **Synthesis of crosslinked HA hydrogels**

Sodium hyaluronate 0.75% (w/v) was dissolved in 1 ml distilled water and then mixed with various final concentrations of 4-arm PEG-amine at 25 mM, 50 mM, 75 mM, 100 mM and 50 mM 0.625% glutaraldehyde (GTA). After complete mixing, N-hydroxysuccinimide (NHS) 15% (w/v) and 1-ethyl-3-(3-dimethylaminopropyl)carbodiimide (EDC) 9% (w/v) were added to initiate the crosslinking (Figure 1A). Consistent with our previous method of hydrogel preparation,<sup>35</sup> spherical-shaped hydrogels were then obtained through pipetting a channel volume of 5  $\mu$ l onto a hydrophobically modified glass slide prepared by layering Teflon™ tape. The spherical-shaped droplets of the reaction mixture were then incubated for 1 h at 37°C to allow complete crosslinking (Figure 1B). After complete fabrication, the HA hydrogels were washed in PBS overnight to remove the un-reactant and then dried and stored at 4°C for further analyses.



### **Optimization of the crosslinking system**

The synthesis of crosslinked HA hydrogels was optimized using different concentrations of 4-arm PEG-amine at 25 mM, 50 mM, 75 mM, 100 mM and 50 mM 0.625% GTA by determining of free carboxyl groups of HA, quantifying of unreacted amine group of PEG and HA hydrogel morphology by scanning electron microscope.

The residual un-crosslinked carboxyl groups of HA were measured by fourier transformed infrared spectroscopy (FTIR). Each hydrogel prepared at different ratios of PEG/HA was dried under vacuum and then studied by FTIR spectrometer (Varian 660-IR, Agilent Technology, Ireland) against a blank KBr pellet background.

A 2,4,6-trinitrobenzene sulfonic acid (TNBSA) assay (Thermo Scientific, USA) was performed to determine the amount of unreacted amine groups of PEG during the coupling reaction. Briefly, 1 mg hydrogel was dissolved in 1 ml reaction buffer of 0.1 M sodium bicarbonate, pH 8.5. Each 200  $\mu$ l sample was mixed with 100  $\mu$ l 0.01% TNBSA and then incubated at 37°C for 2 hours. 100  $\mu$ l 10% solution of SDS and 50  $\mu$ l 1 N HCl was added for every 100  $\mu$ l sample. Samples were run in triplicate and the amount of free amine groups in the hydrogel was determined by measuring the UV absorbance (Varioskan Flash, Thermofisher Scientific, Finland) of the supernatant at 335 nm and compared to a standard curve produced using glycine as a reference.

The surface morphology of different concentrations of crosslinked HA hydrogels was imaged by scanning electron microscopy (SEM). The hydrogels were dehydrated in a series of increasing ethanol concentrations in water and then freeze-dried. Dried samples were gold-coated before being analysed by Hitachi S-4700 SEM operated at 10 kV accelerating voltage.

### **In vitro degradation**

Finally, the optimally crosslinked HA hydrogel was obtained using 75 mM PEG-amine. The hydrogel stability was determined by hydrolytic and enzymatic degradation. Pre-weighed ( $W_1$ ) HA hydrogels were incubated in PBS and hyaluronidase (5 U/ml) respectively at 37°C using a water bath. The degradation medium was replenished with either PBS or a freshly prepared enzyme solution every 2 days. The hydrogels were recovered after 1, 3, 7, 14 and 28 days and dried under vacuum. The dry weight of HA gels ( $W_2$ ) at each time point was measured and the weight-percentage of remaining hydrogels (wt%) was calculated using:

$$\text{wt}\% = \frac{W_1 - W_2}{W_1} \times 100\%$$

### **NP cell isolation**

The discs from T9-S1 spine were isolated from freshly obtained 5-month-old bovine tails that were collected directly after sacrifice from a local slaughterhouse. Soft tissues surrounding the disc (muscles, tendons and ligaments) were manually dissected. The discs were cut into four sagittal sections (4 mm wide) using custom dissection tools. The NP tissues were harvested from each section. Tissues were washed twice with Hanks' Balanced Salt Solution (HBSS) and once using blank high glucose (HG) Dulbecco's modified Eagle's medium (DMEM). NP tissues were digested with 0.19% pronase prepared in HGD MEM media for one hour under agitation at 37°C in a humidified atmosphere of 5% CO<sub>2</sub> and were then centrifuged for five minutes at 1200 rpm. The pellets were washed three times with complete medium to inhibit pronase activity and then were resuspended in 0.025% collagenase type IV (327I U/mL) prepared in complete media. The mixture was incubated under agitation overnight at 37°C in a humidified atmosphere of 5% CO<sub>2</sub>.

The suspensions were filtered through a 70  $\mu\text{m}$  cell strainer and centrifuged for 8 minutes at 1200 rpm. Pellets were washed once and resuspended with complete media. The cells were counted using a haemocytometer and the  $5 \times 10^3$  cells were seeded on four well chambers and  $1 \times 10^4$  cells were seeded on a modified glass surface 24 well cell culture plates.

### **Viability of NP cells**

The cytotoxicity of crosslinked hydrogels at different concentrations of HA 0.75 mg (in 100  $\mu\text{l}$ ) and 1.5 mg (in 200  $\mu\text{l}$ ) was investigated on NP cells at the first passage. Briefly, the  $5 \times 10^3$  cells were seeded on four well chambers and allowed to grow for 1, 3 and 7 days in the presence of crosslinked hydrogels at 37°C in a humidified atmosphere of 5%  $\text{CO}_2$ . The NP cell morphology was observed using Live/Dead<sup>®</sup> staining kit, after which cell metabolic activity was determined using alamarBlue<sup>®</sup> assay.

### **Therapeutic effect of optimally crosslinked 4-arm PEG-amine HA hydrogels in IL-1 $\beta$ induced inflammation model of NP cells**

#### ***In vitro* inflammation model of NP cells**

NP cells ( $1 \times 10^4$ ) were seeded on a modified glass surface 24 well cell culture plate prepared by putting 13 mm sterile glass cover slips onto cell culture well. The cells were grown in complete medium containing DMEM, 10% fetal bovine serum (FBS) and 1% penicillin/streptomycin (P/S) at 37°C in a humidified atmosphere of 5%  $\text{CO}_2$ . After 1 day in culture, the cells were stimulated with IL-1 $\beta$  (10 ng/ml) prepared in complete medium to create an inflammatory milieu to mimic the disease environment of the IVD degeneration.

Subsequently, after 24 h cytokine stimulation, cells were treated with HA hydrogels for 3 and 7 days. The concentration of HA to use in the inflammation study was finalized at 0.75 mg in 100  $\mu$ l (5  $\mu$ l  $\times$  20 gels) based on NP viability results.

### **Analysis of immunoreactivity of IL-1R1 and MyD88**

The protein expression of immunoreactive inflammatory receptors was determined by immunofluorescent staining in inflamed NP cells after a three-day treatment with non-crosslinked HA and crosslinked HA hydrogels. Briefly, normal and inflamed NP cells were incubated with non-crosslinked HA and crosslinked HA hydrogel (0.75 mg in 100  $\mu$ l) in DMEM media supplemented with 10% FBS and 1% P/S. After 3 days' incubation, the modified cell culture plates were transferred from incubator to room temperature. The cells were washed three times with phosphate buffered saline (PBS) 1M for five minutes and then fixed with 3.7% paraformaldehyde (PFA) for 15 minutes. After complete washing with PBS 1M three times for 5 minutes each, antigen retrieval was performed using Triton 0.1% for 5 minutes to permeate the cell membrane. Cells were then washed with PBS 1M three times for 5 minutes and incubated overnight at 4°C with primary rabbit anti-IL1R1 antibody (1:200) and rabbit anti-MyD88 antibody (1:200). After washing with PBS 1M three times for 5 minutes each, cells were incubated with Alexa Flour 488 and Alexa Flour 564 secondary anti-rabbit antibodies respectively at room temperature for 1 hour. The cover slips with cells were carefully removed onto glass slides containing anti-fade mounting medium with 4,6-diamidino-2-phenylindole (DAPI). The slides were protected from light overnight at 4°C and staining for immunoreactive IL-1R1 and MyD88 was observed using a laser confocal microscope (Olympus Fluoview 1000). The mean fluorescence intensity of detectable receptors from three areas of each slide was

further analysed using software imageJ version 1.48 (National Institutes of Health, USA). This experiment was carried out in triplicate.

### **mRNA expression of NGF and BDNF**

Normal and inflamed NP cells were incubated with non-crosslinked HA and crosslinked HA hydrogels (0.75 mg in 100  $\mu$ l) in DMEM media supplemented with 10% FBS and 1% P/S. After a seven-day treatment with HA hydrogels, total RNA was extracted from NP cells in monolayer culture using TRIzol reagent (Invitrogen) and miRNeasy mini kit following the manufacturer's protocol. Total RNA of 100 ng/ $\mu$ l was reverse-transcribed with random primer (Promega) and subsequently with reverse transcriptase (Promega) in a 20  $\mu$ l reaction mixture using PTC DNA Engine™ System (PTC-200, Peltier Thermal Cycler, MJ Research Inc., USA). The cDNA products were amplified using SYBR green PCR Master Mix (Promega) and following specific primers (Table 1). Reactions were conducted in triplicate using StepOnePlus™ Real-Time PCR System (Applied Biosystems®). The results were analysed using the  $2^{-\Delta\Delta C_t}$  method and presented as fold change (relative gene expression) normalized to 18S and basal control.

### **Activation of CD44 receptor**

CD44 activation was determined by investigating protein expression in normal and inflamed NP cells after a three day treatment with non-crosslinked HA and crosslinked HA hydrogels (0.75 mg in 100  $\mu$ l). The modified cell culture plates were removed from the incubator and subject to room temperature before beginning immunofluorescence staining. Cells were washed three times with PBS 1 M for five minutes and fixed with 3.7% PFA for 15 minutes. After washing three times with PBS 1 M for five minutes, antigen retrieval was performed using Triton

0.1%. Cells were then washed with PBS 1 M three times for five minutes and incubated overnight at 4°C with anti-CD44 antibody conjugated with FITC (1:100). After washing with PBS 1M three times, the cells were incubated at room temperature for one hour with rhodamine phalloidin (1:200). The cover slips with cells were carefully removed onto glass slides containing anti-fade mounting medium with DAPI. The slides were protected from the light and kept overnight at 4°C. CD44 was visualized using a laser confocal microscope (Olympus FluoView 1000). The mean fluorescence intensity of detectable receptors from three areas of each slide was quantified using software imageJ version 1.48.

### **Statistical analysis**

Statistical analysis was performed using software GraphPad Prism version 5.00. Data were compared by a one-way analysis of variance (ANOVA) check and multiple pairwise comparisons were carried out using the Bonferroni post-hoc t-test. Statistical significance was set at  $p < 0.05$ .

## **Results**

### **Optimization of crosslinked HA hydrogel**

The carboxyl (C=O) stretch of un-crosslinked carboxyl groups of HA after the crosslinking reaction with 4-arm PEG-amine (Figure 2A) was observed at a peak of 1720 nm. A decrease in absorbance of carboxyl groups at 1720 nm was observed for all the concentrations of 4-arm PEG-amine used for the optimization of HA hydrogel crosslinking. Un-crosslinked residual amine groups in HA hydrogel were estimated by TNBSA have shown significant decrease in amine group concentration. A plateau was reached after 75 mM of 4-arm PEG-amine (Figure

2B); demonstrating maximum crosslinking was achieved at that 4-arm PEG-amine concentration. Furthermore, the surface images of the HA hydrogels presented in Figure 3 with a micro-pits structure were observed in SEM images, when using low concentration PEG-amine. The use of high concentration PEG-amine, however, resulted in the formation of a smooth surface structure.

### **Hydrolytic and enzymatic degradability**

The optimally crosslinked HA hydrogel was determined to be stable in *in vitro* degradation. Hydrogels incubated in PBS showed significant decrease in weight up to 30% after 1 day and were stable thereafter with no significant difference. Alternatively, hydrogels were degraded more in the presence of hyaluronidase at  $44.07\% \pm 2.14\%$ ,  $42.36\% \pm 2.58\%$ ,  $40.89\% \pm 1.79\%$ ,  $43.40\% \pm 0.28\%$ , and  $44.67\% \pm 0.73\%$  after 1, 3, 7, 14 and 28 days' incubation respectively. Hydrogels' degradation was significantly different between PBS and hyaluronidase (Figure 4B).

### **NP cell morphology**

Microscopically, the individual cells and clusters of cells with round morphology were observed in basal control of NP cells after 3 days in normal culture (Figure 5A). In hydrogel treatment at different doses of HA, NP cells maintained a chondrocyte-like rounded shape, and some of the cells showed short cytoplasmic extensions in normal culture (Figure 5A).

### **NP cell viability**

After HA hydrogel treatment containing HA dose (0.75 mg in 100  $\mu$ l), NP cells demonstrated  $94.16\% \pm 4.56\%$  (1 day),  $89.79 \pm 4.42\%$  (3 day),  $88.77 \pm 7.44\%$  (7 day) viability, while doubling

the HA dose (1.5 mg in 200  $\mu$ l) showed  $80.51\% \pm 2.58\%$  (1 day),  $74.08 \pm 4.22\%$  (3 day),  $79.87 \pm 3.64\%$  (7 day) in normal monolayer culture respectively (Figure 5B).

### **Suppression of inflammatory receptor**

Examination of IL1R1 and MyD88 protein expression in basal condition and IL-1 $\beta$  induced inflammation on NP cells with or without a HA hydrogels dose of 0.75 mg (in 100  $\mu$ l) was performed by assessing immunofluorescence staining, illustrated in Figure 6A. It confirms immunoreactivity to IL1R1 and MyD88 as shown by green fluorescence corresponding to IL1R1, co-localized with red fluorescence corresponding to MyD88. Immunoreactive IL1R1 and MyD88 were detectable throughout basal and inflamed NP cells, but were more prominent in inflamed NP cells. Both IL1R1 and MyD88 appeared to be less intense in NP cells treated with crosslinked HA hydrogels than in non-crosslinked HA treatment and IL-1 $\beta$  control groups. The mean values with standard error of the mean ( $\pm$ SEM) fluorescence intensity of detectable immunoreactive IL-1R1 and MyD88 were further analysed to quantify the magnitude of protein expression. Figure 6B demonstrates that fluorescence intensity of IL-1R1 decreased significantly in NP cells with crosslinked hydrogels treatment. A consistent result was particularly noted for MyD88 expression, in which fluorescence intensity was significantly reduced in NP cells after crosslinked and non-crosslinked HA hydrogels treatment (Figure 6C).

### **Down-regulation of neurotrophins**

The expression of NGF and BDNF at the mRNA level in basal condition or inflamed NP cells after treating with or without non-crosslinked HA and crosslinked HA hydrogels was performed by qRT-PCR using cDNA extracted from cell monolayer cultures. Figure 7A indicates that NGF



mRNA was constitutively expressed in basal NP cells and highly up-regulated after being induced by IL-1 $\beta$  (10 ng/ml). However, NGF mRNA expression was down-regulated in all HA treatments and was significantly down-regulated in crosslinked HA hydrogels treatment groups. A pattern similar to BDNF mRNA expression shown in Figure 7B was expressed in basal NP cells. This confirmed that IL-1 $\beta$  up-regulated BDNF mRNA expression in NP cells. Nonetheless, the expression was significantly down-regulated in NP cells after treatment with crosslinked HA hydrogels.

#### **Mechanism of action of HA through binding cell surface receptor of CD44**

To the best of our knowledge, this is the first study to examine cell and hydrogel binding in NP cells by investigating binding of antibody to antigen cell surface receptor CD44 in the basal condition and inflamed NP cells. This was carried out by immunofluorescence staining of the receptors.

Figure 8A represents immunoreactive FITC labelled CD44 co-localized with rhodamine phalloidin (for cellular cytoskeleton). CD44 protein was expressed in basal NP cells and was most intense after treatment with crosslinked HA hydrogels. NP cells bind to crosslinked HA through CD44 (shown with a black arrow). To further analyse the strength of protein expression, the mean value with SEM of fluorescence intensity of expressed immunoreactive CD44 was quantified for each group of HA treatment.

Figure 8B shows a fluorescence intensity of CD44 at almost the same level as that in basal control, IL-1 $\beta$  control and NP cells treated with non-crosslinked HA. However, this intensity was significantly increased in NP cells after treatment with crosslinked HA hydrogels. These results suggest that HA hydrogels bind to NP cells through CD44.

## Discussion

A crosslinked HA hydrogel system was developed in this study to evaluate the therapeutic effect of hydrogels and investigate the binding between cells with hydrogels in an *in vitro* inflammation model on NP cells. The structure of multi-arm PEG-amine was important in optimising the hydrogel crosslinking system. 4-arm PEG-amine in hydrogel has been proved to enhance cell adhesion on the hydrogel surface to support biological properties in the system.<sup>47</sup> It can be easily crosslinked with naturally derived biomaterial such as HA to form biodegradable hydrogels.<sup>48</sup> For this reason, 4-arm PEG-amine was used as a crosslinking agent in this study. HA was covalently crosslinked with 4-arm PEG-amine after the carboxyl group of HA was functionalized using EDC coupling in the presence of NHS to stabilize the intermediate in the crosslinking reaction (Figure 1A). EDC and NHS activated carboxyl groups of HA facilitate the amide bond formation with primary amines of 4-arm PEG-amine. The remaining unreacted carboxyl groups of HA were determined by analysis of the FTIR at peak 1720 nm. The carboxyl groups of HA were decreased as PEG-amine concentration increased (Figure 2A). Similarly, the unreacted amine groups of 4-arm PEG-amine that do not participate in crosslinking reaction were found to decrease with increasing PEG-amine concentration. No further changes occurred after 75 mM PEG-amine, which suggests that the maximum crosslinking was reached at this point (Figure 2B). The microstructure of hydrogel was dependent on the concentration of PEG-amine used in the crosslinking reaction. Surface morphology SEM images display a micro-pits structure to a smooth surface layer at lower to higher concentration PEG-amine (Figure 3). These surface morphology changes are probably due to the sufficient crosslinking reaction.

The optimally crosslinked HA hydrogels was determined when using 75 mM PEG-amine. 3D sphere shape of these hydrogel was obtained when apply on hydrophobicity surface at room

temperature (Figure 4A a) and maintained physical structure after complete crosslinking at 37°C (Figure 4A b). Hydrogel was also stable to the hydrolytic process in PBS and showed resistance to enzymatic degradation over 28 days (Figure 4B). Physiologically, HA is degraded predominantly by an enzymatic reaction through hyaluronidase.<sup>49</sup> The results of this finding may be due to the use of PEG in the crosslinking system that can maintain the *in vitro* degradation rate of hydrogels. Therefore, in the present study, we were able to formulate crosslinked HA hydrogels by controlling the degradation profile that are suitable for targeted controlled release drugs or other therapeutic molecules in NP regeneration.

At a cellular level, the clustering of NP cells with chondrocyte-like round shape was observed in basal control. With hydrogel treatment of 0.75 mg (in 100 µl) and 1.5 mg (in 200 µl) doses of HA, the cells maintained round morphology as normal and some of cells adopted a slightly fibroblastic-shape with short cytoplasmic extensions after 3 days culture (Figure 5A). This appears to be because of the binding with HA hydrogels,<sup>36</sup> and the presence of oxygen in the cell culture system. Additionally, no statistical difference in metabolic activity of NP cells was observed after crosslinked HA hydrogel treatment (Figure 5B). This indicates no cytotoxicity was occurred. Our recent results were supported by previous studies showing that HA/type II collagen hydrogel maintained NP cell phenotype<sup>43</sup> and did not influence NP cell viability.<sup>34</sup>

Apart from the physical properties of hydrogel, HA with a different molecular weight affects cellular responses such as cell adhesion, migration, proliferation and also maintains tissue structure.<sup>36</sup> In healthy tissue, HA presents high molecular weight (HMw) with an average  $\sim 10^7$  Da which can maintain tissue integrity and thus suppress the inflammatory response.<sup>50</sup> In this study, IL-1 $\beta$  was used to create an inflammation microenvironment of NP cells since IL-1 $\beta$  is one of main pro-inflammatory cytokine significantly increased in gene and protein expression<sup>11</sup>

that promotes matrix degradation in symptomatic disc degeneration.<sup>51</sup> These current results demonstrated that the inflammatory receptor of IL-1R1 and MyD88 were highly expressed in NP cells after being stimulated by IL-1 $\beta$ . In fact, IL-1 $\beta$  is known to control the inflammatory processes by activating receptor IL-1R1 and IL-1R antagonist.<sup>13</sup> However, after HA hydrogel treatment, these receptors were suppressed at three days in culture (Figure 6). Other supported findings showed that the use of HMw HA in the case of inflammation and tissue injury is through blocking neutrophil and macrophage infiltration in sepsis induced lung injury,<sup>52</sup> inhibiting phagocytosis of peritoneal macrophages,<sup>53</sup> decreasing production of pro-inflammatory cytokines (IL-1 $\beta$  and IL-6) and migration of macrophages in a post-laminectomy rat model.<sup>54</sup>

The inflammatory process also induces neuronal sensitization of nociceptors that can increase synaptic conduction and result in pain sensation. The pro-inflammatory cytokine such as IL-1 $\beta$  is associated with the mechanism of nociception<sup>29</sup> by correlating the local production of neurotrophins and innervation of nociceptive nerve fibres into the disc. IL-1 $\beta$  induces neurotrophin expression of NGF and BDNF, resulting in innervation of human disc samples.<sup>17,15</sup> Our current results show that NGF gene was expressed in basal NP cells and greatly increased regulation after being stimulated by IL-1 $\beta$ . These findings are supported by other studies and indicate that NGF-dependent neurons play a key role in inflammatory pain responses. In dorsal root ganglion (DRG), neurons innervating the disc, neuropeptides or markers for NGF-dependent neurons such as substance P (SP) and CGRP were mainly localised in small DRG neurons which are nociceptive neurons.<sup>55</sup> As with NGF, BDNF mRNA expression also up-regulated after being treated by IL-1 $\beta$ . BDNF is known a central nervous system modulator of nociception by binding to full-length receptor tropomyosin-related kinase B (trkB.FL).<sup>56</sup> Conversely, both NGF and BDNF mRNA expression was down-regulated in all HA treatment and significantly down-

regulated in crosslinked HA hydrogel treatment (Figure 7). These findings are supported by a previous study in which HA effectively reduced pain in osteoarthritic patients<sup>40</sup> and promoted an analgesic effect by activating the opioid receptor.<sup>57</sup>

HA is known to bind to a specific cell surface receptor notably to CD44, that modulates cellular signaling in regulating cell adhesion, growth, survival, migration and differentiation and HA metabolism.<sup>58,59</sup> The presence of HA crosslinking network functions as an anti-inflammatory cascade in response to tissue inflammation and is also mediated through CD44.<sup>46</sup> Here, we demonstrated the immuno-reactivity of CD44 receptor in normal and inflamed NP cells treated with non-crosslinked HA and crosslinked HA hydrogels. However, it was increased significantly in NP cells after treating with crosslinked HA hydrogels (Figure 8). These results suggest that NP cells bind to the crosslinked HA hydrogels through CD44 and interfere pro-inflammatory cytokines binding to their receptors.<sup>46</sup> It has previously been shown that this HA crosslinking network interacts with mononuclear leukocytes through CD44 in response to viral infection.<sup>60</sup> Furthermore, the presence of HA in crosslinked form also stabilises the ECM during ovulation and inflammation, regulates the hydrodynamic effect in the synovial joint, prevents loss of matrix components and thus promotes tissue repair.<sup>46</sup>

The possible protective mechanism of crosslinked HA hydrogels is summarized in Figure 9. Nuclear factor-kappa B (NF- $\kappa$ B) is the major intracellular signalling pathway in mediating the molecular event for pathogenesis of disc degeneration. In the case of inflammation and pain, IL-1 $\beta$  is a pro-inflammatory mediator known to stimulate activation of NF- $\kappa$ B pathway in disc cells. Basically, IL-1 $\beta$  binds to IL-1R1 as part of the MyD88 complex. The active MyD88 induces signal transduction of I $\kappa$ B kinase (IKK) formation. Once IKK becomes activated and phosphorylates I $\kappa$ B to specific serine residues, this results in degradation. I $\kappa$ B degradation causes

NF- $\kappa$ B to undergo translocation into the nucleus and subsequently bind to cDNA sequence that transcribes for specific gene expression.<sup>6</sup> Here, IL-1 $\beta$  induces activation of NF- $\kappa$ B to up-regulate transcription gene expression of pain mediators such as NGF and BDNF. However, in the hydrogel system, this crosslinked HMw HA provides a protective mechanism through binding of the CD44 receptor on NP cells. Consequently, it prevents the pro-inflammatory cytokines from binding to their receptors and inhibits transcription gene expression of neurotrophins to protect NP cells from further inflammation.

## **Conclusions**

The formulated crosslinked HMw HA hydrogels were stable, maintained a 3D structure and demonstrated enzymatic resistance to degradation. No cytotoxicity of hydrogels was observed in NP cells after 7 days in culture. Additionally, HA hydrogels showed a therapeutic effect by suppressing the inflammatory receptor of IL-1R1, MyD88 and down-regulated NGF and BDNF gene expression. These crosslinked HA hydrogels also bind to the CD44 receptor of NP cells and subsequently prevent binding of pro-inflammatory cytokines to their receptors to protect NP cells in response to inflammatory insults. Therefore, this biophysical and anti-inflammatory effect of HA-based hydrogel provides a suitable microenvironment for NP regeneration.

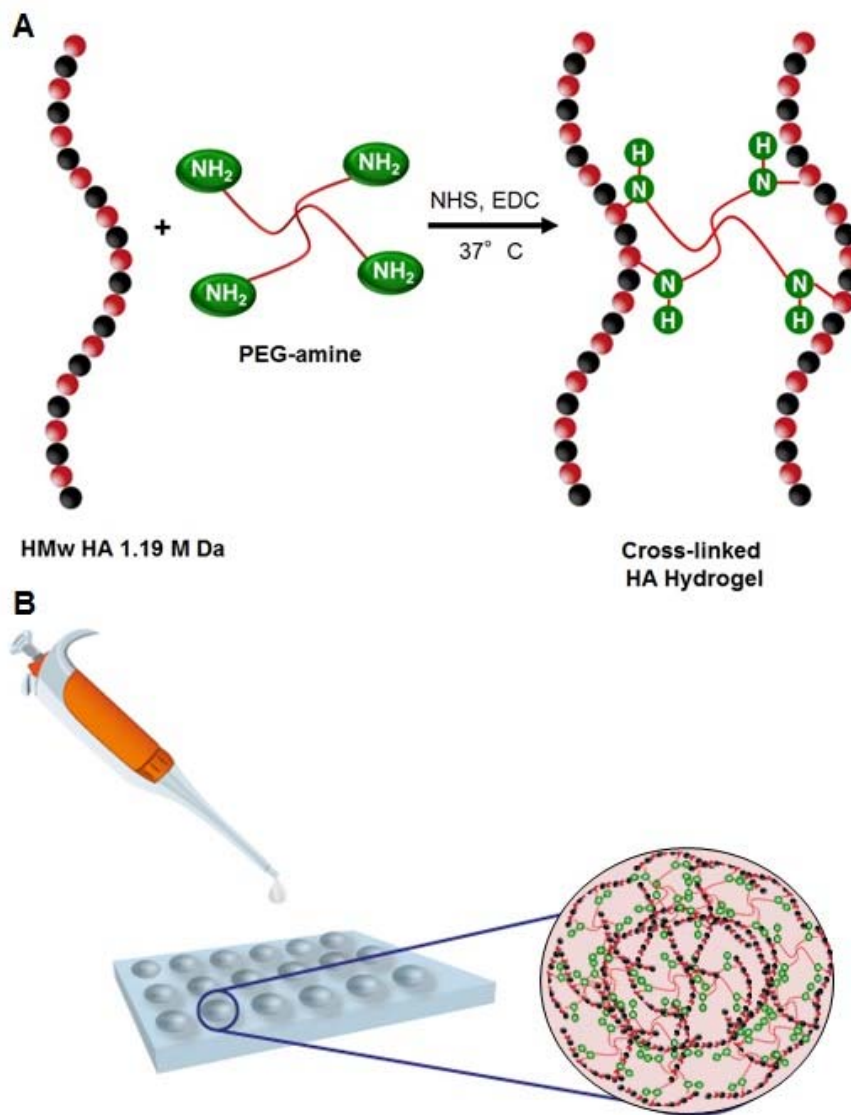


**Figure 1.** Schematic representation of crosslinked HA hydrogel system. (A) Crosslinking of high molecular weight hyaluronic acid and 4-arm PEG-amine. The succinimidyl groups of PEG-amine react with the amine groups on the HA molecules after carboxyl groups are functionalized with EDC and NHS. (B) 3D spherical shaped hydrogel preparation. 5  $\mu$ l of mixed gel solution containing HA, PEG-amine, EDC and NHS was dropped onto hydrophobic modified surface through pipette channel and incubated at 37°C for 1 h to allow crosslinking reaction to complete.

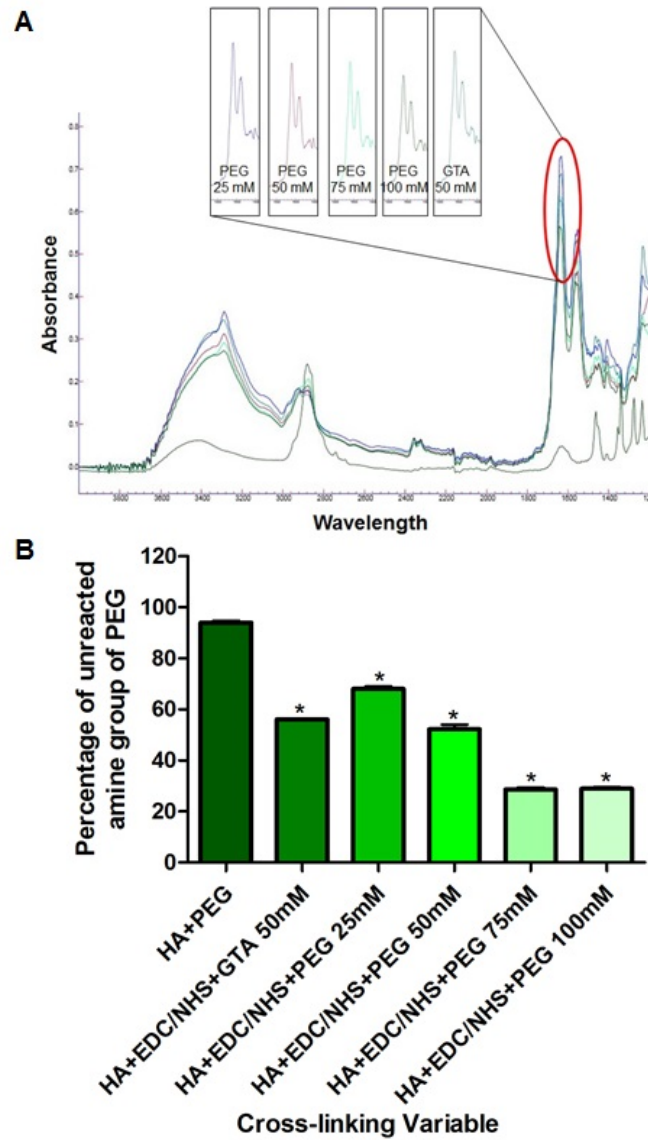


**Figure 2.** Optimization of crosslinking system using different concentrations 4-arm PEG-amine of 25, 50, 75 and 100 mM. GTA was used as a control. (A) Determination of un-crosslinked carboxyl groups of HA after crosslinking reaction at a peak of 1720 nm, corresponding to the C=O stretch from the acid group. A decreasing pattern of peak in carboxyl groups as the PEG concentration increased. (B) Quantification of residual unreacted amine groups of PEG after crosslinkage. Free amine group was decreased with increasing of PEG concentration.



\*Significant statistical different for different concentrations of PEG-amine. ( $n = 3$ , one-way ANOVA,  $p < 0.05$ ). Data presented as the mean  $\pm$  standard error of the mean.

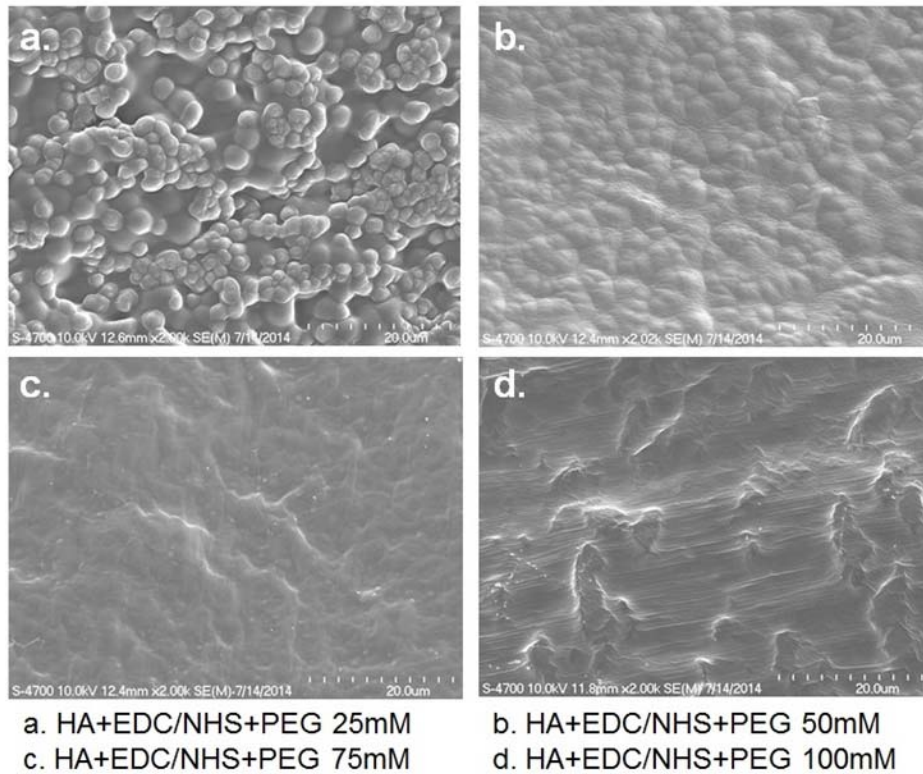


**Figure 3.** Physical properties of hydrogels at different concentrations 4-arm PEG-amine: 25, 50, 75 and 100 mM. GTA was used as a control. Surface morphology of the crosslinked HA hydrogels was presented as a micro-pits structure to a smooth surface layer at lower to higher concentrations of PEG-amine ( $n = 3$ , one-way ANOVA,  $p < 0.05$ ). Data presented as the mean  $\pm$  standard error of the mean.

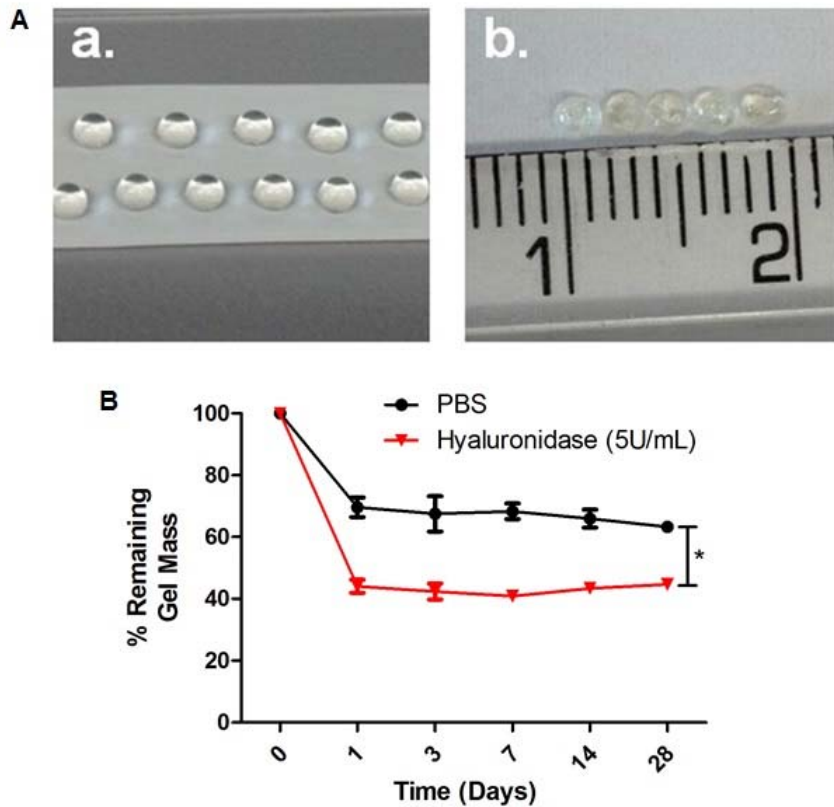


**Figure 4.** Characterization of optimal 75 mM 4-arm PEG HA hydrogels. (A) Spherical-shaped hydrogels were obtained on modified hydrophobic surface using Teflon tape at room temperature (a) and the gels maintained a 3D spherical shape after complete crosslinking at 37°C (b). (B) Over 70% and 40% remaining gel mass of hydrogels in PBS and hyaluronidase over 28 days respectively \*Significant differences were noted between the different groups ( $n = 3$ , one-way ANOVA,  $p < 0.05$ ). Data presented as the mean  $\pm$  standard error of the mean.

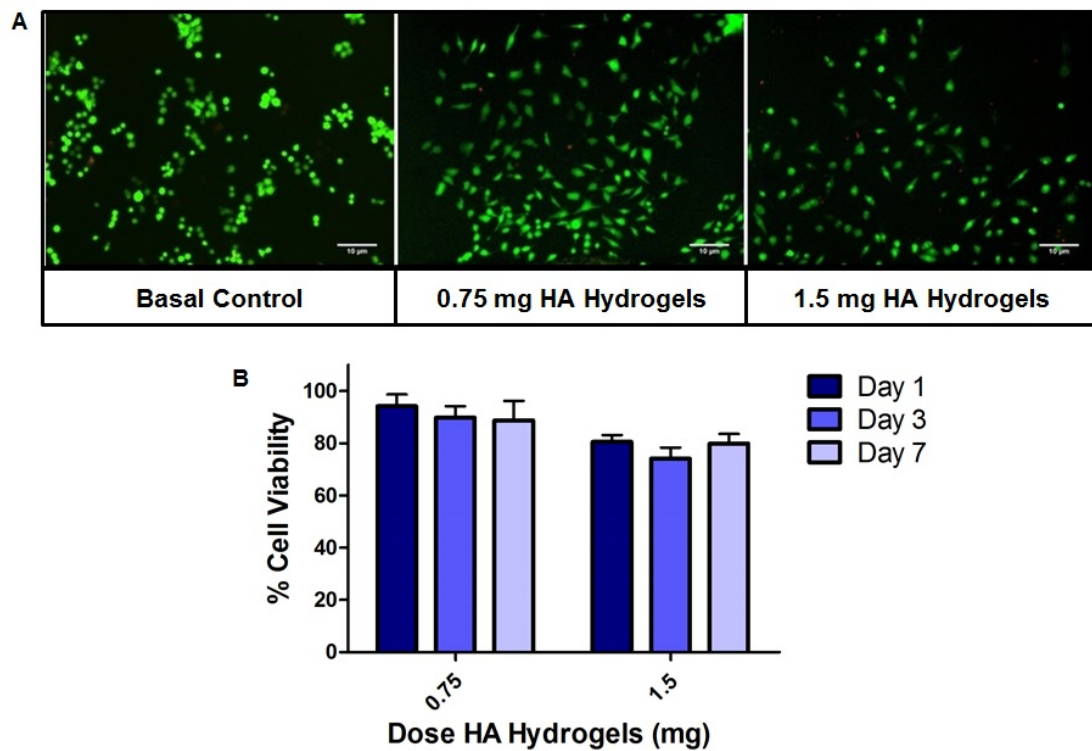


**Figure 5.** Viability study of NP cells after HA hydrogel treatment. (A) NP cell morphology in hydrogels containing different doses of HA stained by LIVE/DEAD® assay after 3 days in culture. Viable cells appear in green (calcein staining) and dead cells in red (ethidium bromide staining). (B) NP cells showed over 88% and 74% viability in the treatment of 0.75 mg (in 100  $\mu$ l) and 1.5 mg (in 200  $\mu$ l) crosslinked HA hydrogels respectively as measured by alamarBlue® assay. There was no significant difference between the groups ( $n = 3$ , one-way ANOVA,  $p < 0.05$ ). Data presented as the mean  $\pm$  standard error of the mean.

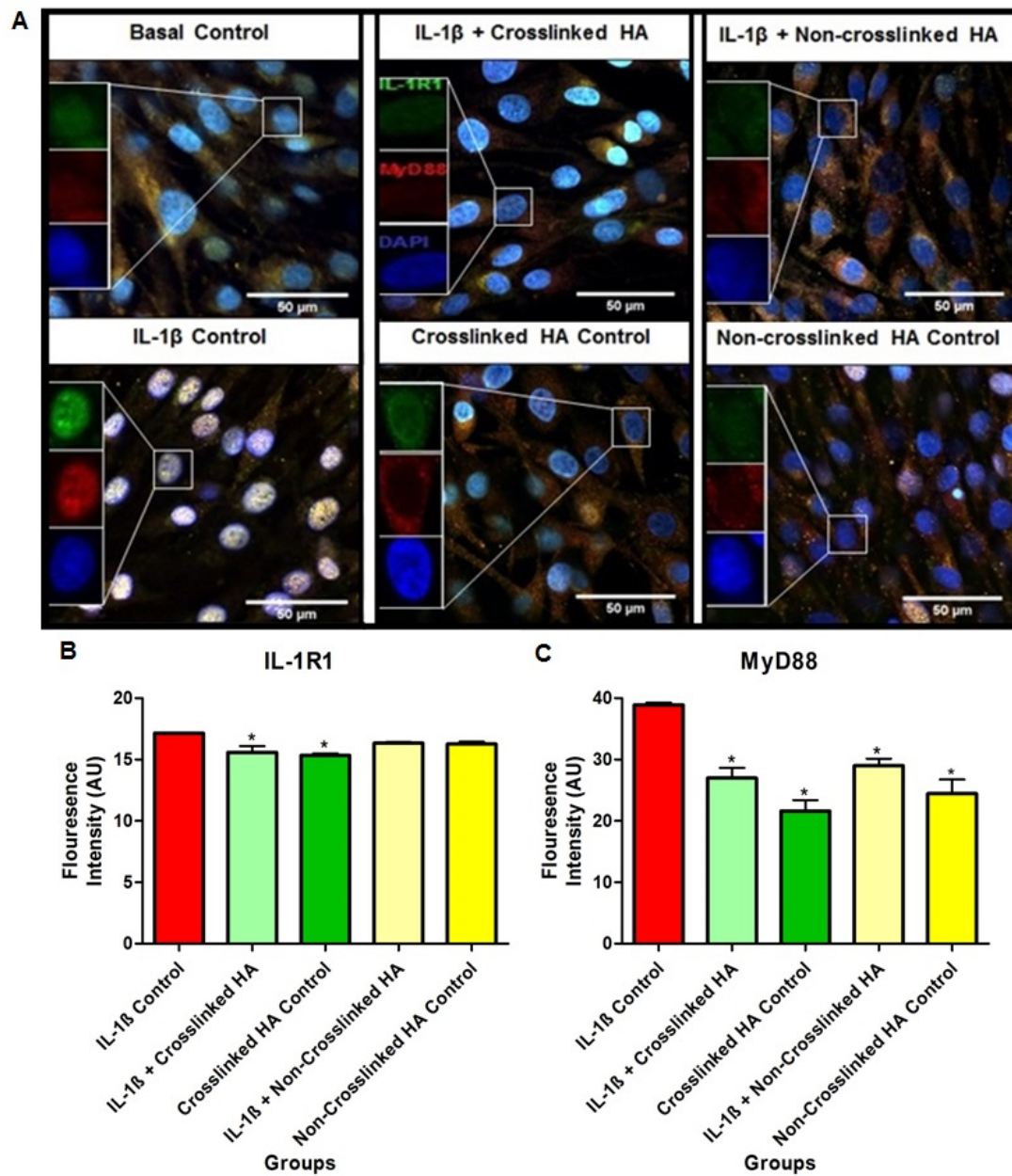


**Figure 6.** Expression of IL-1R1 and MyD88 in NP cells after HA treatment. (A) Confocal micrograph showing IL-1R1 (green) co-localized with MyD88 (red) in IL-1 $\beta$  induced inflammation and normal NP cells in the treatment of 0.75 mg (in 100  $\mu$ l) crosslinked and non-crosslinked HA after 3 days in culture. (B) Mean fluorescence intensity showing IL-1R1 receptor was significantly suppressed in the treatment of crosslinked HA hydrogels compared to IL-1 $\beta$

control group. (C) Mean fluorescence intensity of MyD88 significantly decreased after being treated with HA compared to IL-1 $\beta$  control group. \*Significant differences were noted between the different groups ( $n = 3$ , one-way ANOVA,  $p < 0.05$ ). Data presented as the mean  $\pm$  standard error of the mean.

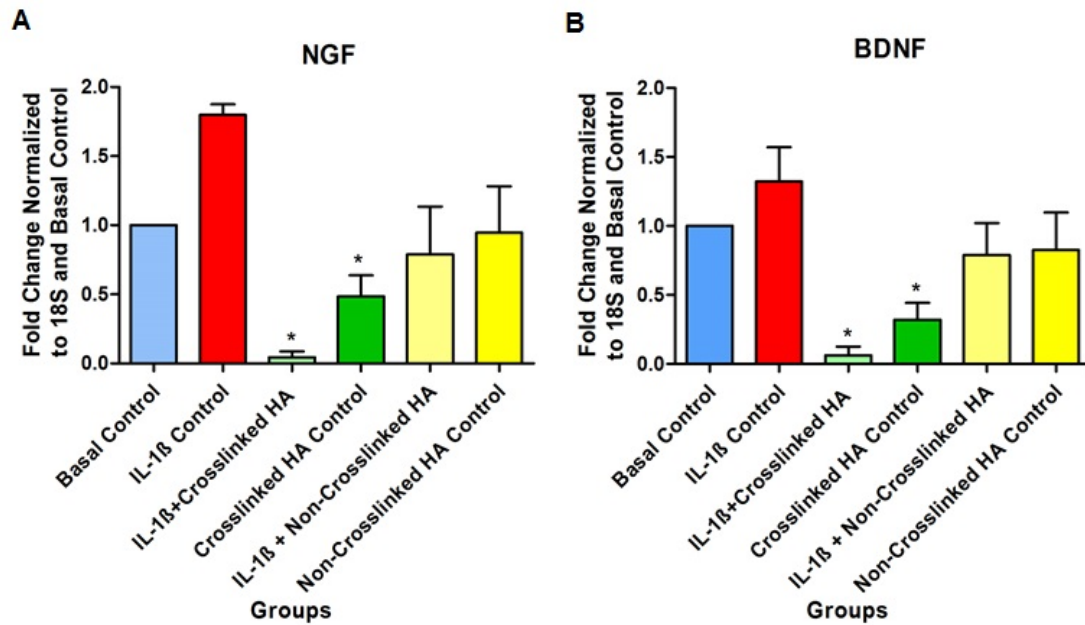


**Figure 7.** Effect of HA treatment on neurotrophin mRNA expression of NP cells normalized to 18S and basal control. Histograms illustrating the fold change of (A) nerve growth factor and (B) brain derived neurotrophic factor down-regulated in IL-1 $\beta$  induced inflammation and normal NP cells in the treatment of crosslinked HA hydrogels. \*Significant differences were noted between the different groups ( $n = 3$ , one-way ANOVA,  $p < 0.05$ ). Data presented as the mean  $\pm$  standard error of the mean.

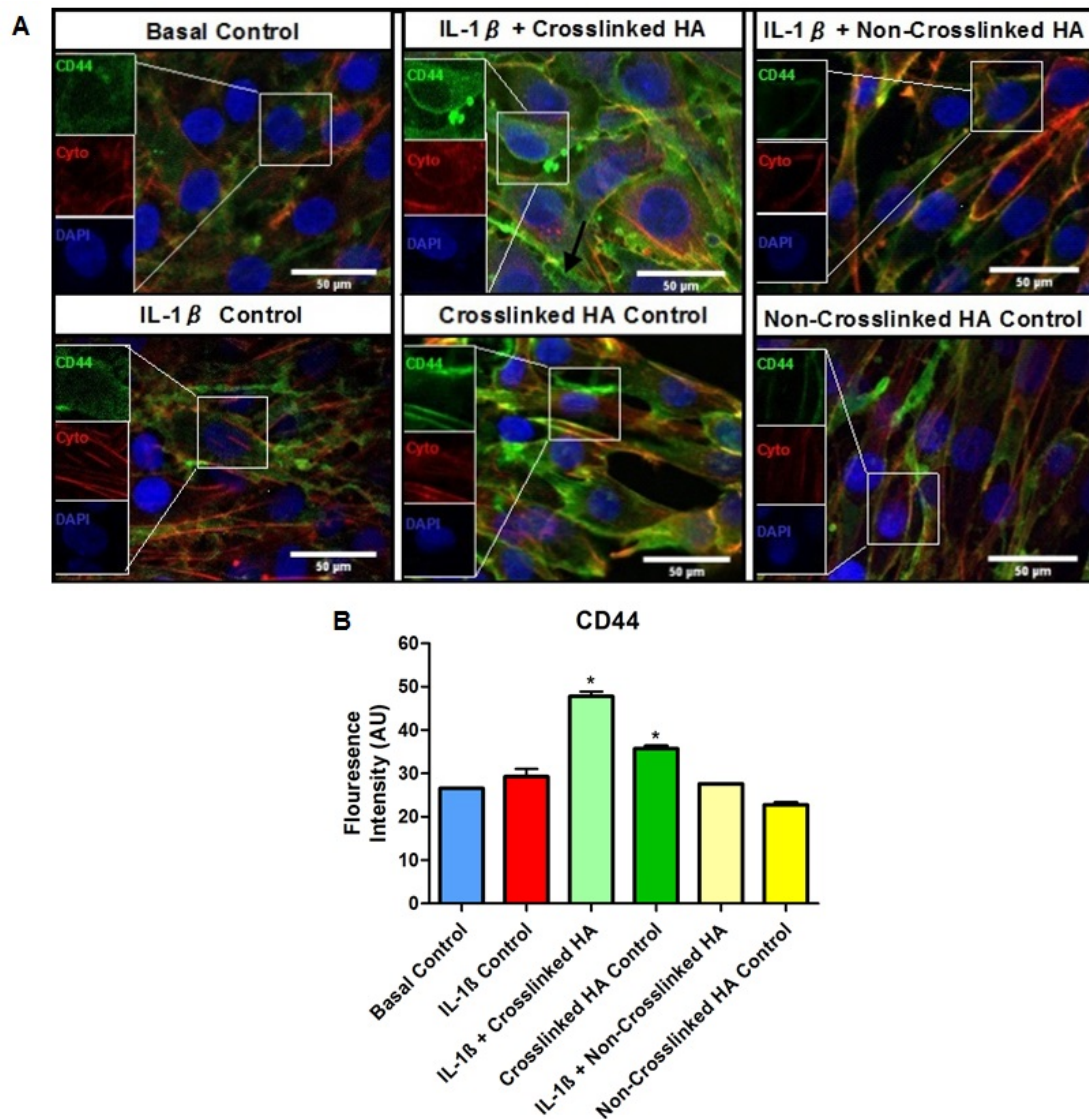


**Figure 8.** Activation of CD44 in NP cells after HA treatment. (A) Confocal micrograph showing distribution and co-localization of CD44 (green) and cellular cytoskeleton (red) in IL-1 $\beta$  induced inflammation and normal NP cells in the treatment of 0.75 mg (in 100  $\mu$ l) crosslinked hydrogels and non-crosslinked HA after 3 days culture. NP cells bind to a cable-like structure of crosslinked HA through CD44, which are shown by the black arrow. (B) Histogram illustrating mean fluorescence intensity of CD44 receptor significantly activated in crosslinked HA hydrogels treatment compared to IL-1 $\beta$  control group. \*Significant differences were noted

between the different groups ( $n = 3$ , one-way ANOVA,  $p < 0.05$ ). Data presented as the mean  $\pm$  standard error of the mean.

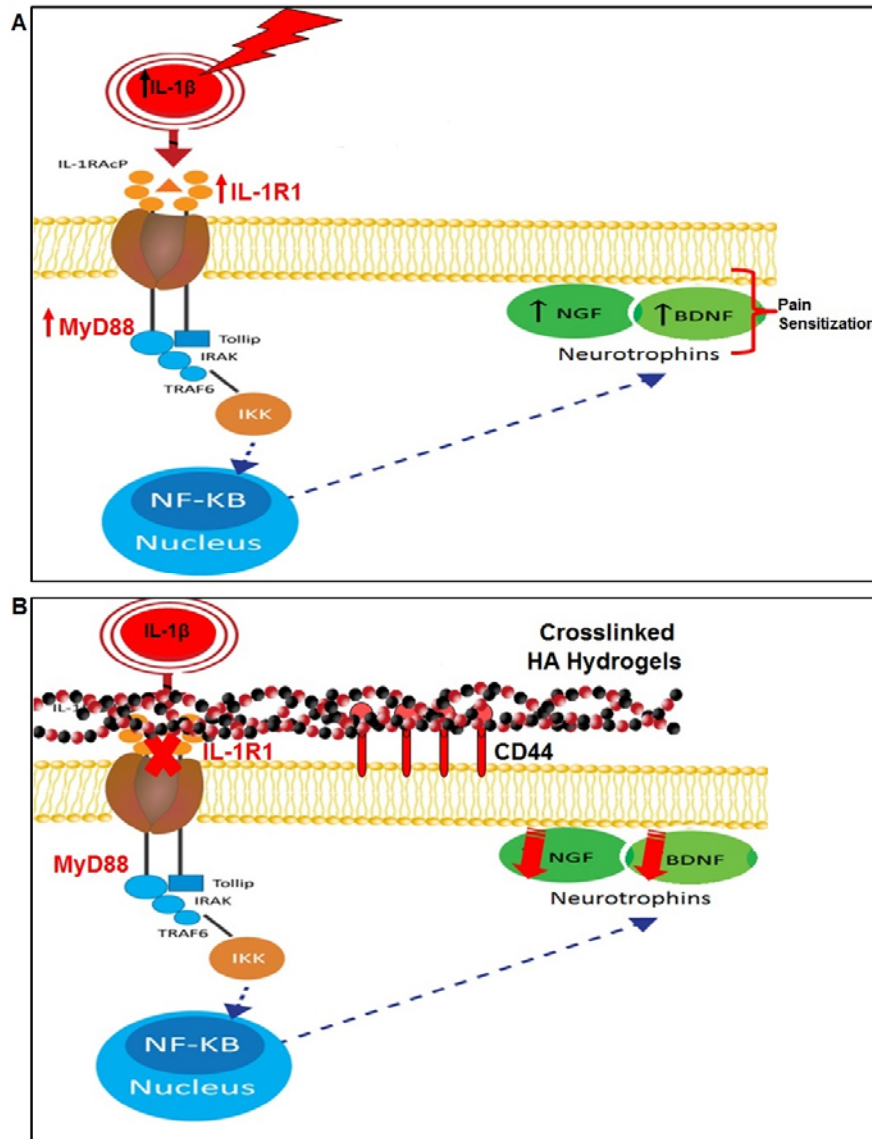


**Figure 9.** Schematic representation of possible protective mechanism of crosslinked HA hydrogels in response to inflammation. (A) At a molecular level, IL-1 $\beta$  binds to IL-1R1 to form MyD88 complex. The active MyD88 induces signal transduction of IKK and transcription factor of NF- $\kappa$ B to up-regulate neurotrophins of NGF and BDNF. The presence of these neurotrophins can stimulate innervation of nociceptive nerve fibres and lead to pain. (B) In the hydrogel

system, these crosslinked HA bind to CD44 receptor of NP cells. Consequently, it prevents pro-inflammatory cytokines from binding to their receptors and inhibits transcription of neurotrophins to protect NP cells from further inflammation.

Gene	Primer sequence		Base pair
	Forward	Reverse	
NGF	5' AAG GGC AAG GAG GTG ATG 3'	5' CTT GAC GAA GGT GTG GGT 3'	18
BDNF	5' TAT TGG CTG GCG GTT CAT AC 3'	5' TCC CTT CTG GTC ATG GAA ATG 3'	20
18S	5' TCA ACA CGG GAA ACC TCA C 3'	5' CGC TCC ACC AAC TAA GAA C 3'	19

**Table 1.** Primers utilized in qRT-PCR analysis.

## ASSOCIATED CONTENT

### Supporting Information

Additional data on viability of adipose derived stem cells (ADSCs) in the presence of crosslinked HA hydrogels, showing that ADSCs were dispersed individually as normal as basal control group. Over 85% and 78% cell metabolic activity in presence of 0.75 mg (in 100  $\mu$ l) and 1.5 mg (in 200 $\mu$ l) hydrogels after 1, 3 and 7 days in culture respectively. This material is available free of charge via the Internet at <http://pubs.acs.org>.



## AUTHOR INFORMATION

### **Corresponding Author**

\*Tel. +353(0)91 492758. E-mail: abhay.pandit@nuigalway.ie.

### **Present Addresses**

†If an author's address is different than the one given in the affiliation line, this information may be included here.

### **Author Contributions**

The manuscript was written with contributions from all authors. All authors have given approval to the final version of the manuscript. ‡These authors contributed equally.

### **Funding Sources**

Majlis Amanah Rakyat (MARA) Malaysia.

## ACKNOWLEDGMENTS

The authors would like to thank Majlis Amanah Rakyat (MARA) Malaysia (Grant no: ROG1112) and the DiscMat Collaborative Research Center AO Foundation for providing financial support to this project. The authors would like to acknowledge Dr Oliver Carroll for his technical support, Mr Anthony Sloan for editorial assistance with this manuscript and Mr Maciej Doczyk for his help with diagrams.

## ABBREVIATIONS

IL-1R1, interleukin-1 receptor 1; IL-1RA, interleukin-1 receptor Antagonist; MyD88, myeloid differentiation primary response 88; MMP-3, matrix metalloproteinase-3; MMP-13, matrix metalloproteinase-13; ADAMTS-4, A disintegrin and metalloproteinase with thrombospondin motifs 4; TNF- $\alpha$ , tumor necrosis factor alpha; NF- $\kappa$ B, nuclear factor kappa-light-chain-enhancer of activated B cells; CD44, Cluster of Differentiation 44; EDC, 1-Ethyl-3-(3-dimethylaminopropyl)carbodiimide; NHS, N-Hydroxysuccinimide; PEG, Poly(ethylene glycol); T9, 9th thoracic vertebra; S1, 1st sacral vertebra; FITC, Fluorescein isothiocyanate.

## REFERENCES

- (1) Takahashi, K.; Aoki, Y.; Ohtori, S. Resolving Discogenic Pain. *Eur. Spine J.* **2008**, *17 Suppl 4*, 428–431.
- (2) Peng, B.; Hao, J.; Hou, S.; Wu, W.; Jiang, D.; Fu, X.; Yang, Y. Possible Pathogenesis of Painful Intervertebral Disc Degeneration. *Spine (Phila. Pa. 1976)*. **2006**, *31*, 560–566.
- (3) Majid, K.; Truumees, E. Epidemiology and Natural History of Low Back Pain. *Semin. Spine Surg.* **2008**, *20*, 87–92.
- (4) Driscoll, T.; Jacklyn, G.; Orchard, J.; Passmore, E.; Vos, T.; Freedman, G.; Lim, S.; Punnett, L. The Global Burden of Occupationally Related Low Back Pain: Estimates from the Global Burden of Disease 2010 Study. *Ann. Rheum. Dis.* **2014**, *73*, 975–981.
- (5) Luoma, K.; Riihimäki, H.; Luukkonen, R.; Raininko, R.; Viikari-Juntura, E.; Lamminen, a. Low Back Pain in Relation to Lumbar Disc Degeneration. *Spine (Phila. Pa. 1976)*. **2000**, *25*, 487–492.
- (6) Wuertz, K.; Vo, N.; Kletsas, D.; Boos, N. Inflammatory and Catabolic Signalling in Intervertebral Discs: The Roles of NF- $\kappa$ B and MAP Kinases. *Eur. Cell. Mater.* **2012**, *23*, 103–119; discussion 119–120.
- (7) Chou, R.; Huffman, L. H. Medications for Acute and Chronic Low Back Pain : A Review of the Evidence for an American Pain Society / American College of Physicians Clinical Practice Guideline. *Ann. Intern. Med.* **2007**, *147*, 505–514.

- (8) Xuemei, L.; Ricardo, P.; Lesley H., C.; Lloyd A., H. Prescription of Nonsteroidal Anti-Inflammatory Drugs and Muscle Relaxants for Back Pain in the United States. *Spine (Phila. Pa. 1976)*. **2004**, *29*, E531–E537.
- (9) David A., L.; James J., H.; John A., B. Adjacent Segment Degeneration Following Spinal Fusion for Degenerative Disc Disease. *Bull. NYU Hosp. Jt. Dis.* **2007**, *65*, 29–36.
- (10) Krock, E.; Rosenzweig, D. H.; Chabot-Doré, A.-J.; Jarzem, P.; Weber, M. H.; Ouellet, J. a; Stone, L. S.; Haglund, L. Painful, Degenerating Intervertebral Discs up-Regulate Neurite Sprouting and CGRP through Nociceptive Factors. *J. Cell. Mol. Med.* **2014**, *18*, 1213–1225.
- (11) Le Maitre, C. L.; Hoyland, J. A.; Freemont, A. J. Catabolic Cytokine Expression in Degenerate and Herniated Human Intervertebral Discs: IL-1beta and TNFalpha Expression Profile. *Arthritis Res. Ther.* **2007**, *9*, R77.
- (12) Kepler, C. K.; Ponnappan, R. K.; Tannoury, C. a; Risbud, M. V; Anderson, D. G. The Molecular Basis of Intervertebral Disc Degeneration. *Spine J.* **2013**, *13*, 318–330.
- (13) Le Maitre, C. L.; Freemont, A. J.; Hoyland, J. A. The Role of Interleukin-1 in the Pathogenesis of Human Intervertebral Disc Degeneration. *Arthritis Res. Ther.* **2005**, *7*, R732–R745.
- (14) Wuertz, K.; Haglund, L. Inflammatory Mediators in Intervertebral Disk Degeneration and Discogenic Pain. *Glob. spine J.* **2013**, *3*, 175–184.
- (15) Abe, Y.; Akeda, K.; An, H. S.; Aoki, Y.; Pichika, R.; Muehleman, C.; Kimura, T.; Masuda, K. Proinflammatory Cytokines Stimulate the Expression of Nerve Growth Factor by Human Intervertebral Disc Cells. *Spine (Phila. Pa. 1976)*. **2007**, *32*, 635–642.
- (16) Abe, Y.; Aoki, Y.; Kimura, T.; Masuda, K. Proinflammatory Cytokines Stimulate the Expression of Nerve Growth Factor by Human Intervertebral Disc Cells. *Spine (Phila. Pa. 1976)*. **2007**, *32*, 635–642.
- (17) Lee, J. M.; Song, J. Y.; Baek, M.; Jung, H.-Y.; Kang, H.; Han, I. B.; Kwon, Y. Do; Shin, D. E. Interleukin-1 $\beta$  Induces Angiogenesis and Innervation in Human Intervertebral Disc Degeneration. *J. Orthop. Res.* **2011**, *29*, 265–269.
- (18) Aoki, Y.; An, H. S.; Takahashi, K.; Miyamoto, K.; Lenz, M. E.; Moriya, H.; Masuda, K. Axonal Growth Potential of Lumbar Dorsal Root Ganglion Neurons in an Organ Culture System: Response of Nerve Growth Factor-Sensitive Neurons to Neuronal Injury and an Inflammatory Cytokine. *Spine (Phila. Pa. 1976)*. **2007**, *32*, 857–863.
- (19) Gingras, M.; Bergeron, J.; Durham, H. D. In Vitro Development of a Tissue-Engineered Model of Peripheral Nerve Regeneration to Study Neurite Growth. *FASEB J.* **2003**, 2124–2126.

- (20) Freemont, A. J.; Watkins, A.; Le Maitre, C.; Baird, P.; Jeziorska, M.; Knight, M. T. N.; Ross, E. R. S.; O'Brien, J. P.; Hoyland, J. A. Nerve Growth Factor Expression and Innervation of the Painful Intervertebral Disc. *J. Pathol.* **2002**, *197*, 286–292.
- (21) Diamond, J.; Coughlin, M.; Macintyre, L.; Holmes, M. Evidence That Endogenous IU Nerve Growth Factor Is Responsible for the Collateral Sprouting, but Not the Regeneration, of Nociceptive Axons in Adult Rats. *Proc. Natl. Acad. Sci. USA* **1987**, *84*, 6596–6600.
- (22) Clifford J., W.; Qing-Ping, M.; Andrew, A.; Stephen, P. Peripheral Cell Types Contributing to the Hyperalgesic Action of Nerve Growth Factor in Inflammation. *J. Neurosci.* **1996**, *16*, 2716–2723.
- (23) Snider, W. D.; McMahon, S. B. Tackling Pain at the Source: New Ideas about Nociceptors. *Neuron* **1998**, *20*, 629–632.
- (24) Kirschenbaum, B.; Goldman, S. a. Brain-Derived Neurotrophic Factor Promotes the Survival of Neurons Arising from the Adult Rat Forebrain Subependymal Zone. *Proc. Natl. Acad. Sci. U. S. A.* **1995**, *92*, 210–214.
- (25) Li, C.Q.; Xu, J.M.; Liu, D.; Zhang, J.-Y.; Dai, R.P. Brain Derived Neurotrophic Factor (BDNF) Contributes to the Pain Hypersensitivity Following Surgical Incision in the Rats. *Mol. Pain* **2008**, *4*, 27.
- (26) Hellard, D.; Brosenitsch, T.; Fritsch, B.; Katz, D. M. Cranial Sensory Neuron Development in the Absence of Brain-Derived Neurotrophic Factor in BDNF/Bax Double Null Mice. *Dev. Biol.* **2004**, *275*, 34–43.
- (27) Merighi, A.; Salio, C.; Ghirri, A.; Lossi, L.; Ferrini, F.; Betelli, C.; Bardoni, R. BDNF as a Pain Modulator. *Prog. Neurobiol.* **2008**, *85*, 297–317.
- (28) Gruber, H. E.; Ingram, J. A; Hoelscher, G.; Zinchenko, N.; Norton, H. J.; Hanley, E. N. Brain-Derived Neurotrophic Factor and Its Receptor in the Human and the Sand Rat Intervertebral Disc. *Arthritis Res. Ther.* **2008**, *10*, R82.
- (29) De Souza Grava, A. L.; Ferrari, L. F.; Defino, H. L. a. Cytokine Inhibition and Time-Related Influence of Inflammatory Stimuli on the Hyperalgesia Induced by the Nucleus Pulposus. *Eur. Spine J.* **2012**, *21*, 537–545.
- (30) Purmessur, D.; Cornejo, M. C.; Cho, S. K.; Roughley, P. J.; Linhardt, R. J.; Hecht, A. C.; Iatridis, J. C. Intact Glycosaminoglycans from Intervertebral Disc-Derived Notochordal Cell Conditioned Media Inhibits Neurite Growth While Maintaining Neuronal Cell Viability. *Spine J.* **2015**.
- (31) Frith, J. E.; Cameron, A. R.; Menzies, D. J.; Ghosh, P.; Whitehead, D. L.; Gronthos, S.; Zannettino, A. C. W.; Cooper-White, J. J. An Injectable Hydrogel Incorporating

- Mesenchymal Precursor Cells and Pentosan Polysulphate for Intervertebral Disc Regeneration. *Biomaterials* **2013**, *34*, 9430–9440.
- (32) Sakai, D.; Mochida, J.; Iwashina, T.; Hiyama, A.; Omi, H.; Imai, M.; Nakai, T.; Ando, K.; Hotta, T. Regenerative Effects of Transplanting Mesenchymal Stem Cells Embedded in Atelocollagen to the Degenerated Intervertebral Disc. *Biomaterials* **2006**, *27*, 335–345.
- (33) Peroglio, M.; Eglin, D.; Benneker, L. M.; Alini, M.; Grad, S. Thermoreversible Hyaluronan-Based Hydrogel Supports in Vitro and Ex Vivo Disc-like Differentiation of Human Mesenchymal Stem Cells. *Spine J.* **2013**, *13*, 1627–1639.
- (34) Collin, E. C.; Grad, S.; Zeugolis, D. I.; Vinatier, C. S.; Clouet, J. R.; Guicheux, J. J.; Weiss, P.; Alini, M.; Pandit, A. S. An Injectable Vehicle for Nucleus Pulposus Cell-Based Therapy. *Biomaterials* **2011**, *32*, 2862–2870.
- (35) Fontana, G.; Srivastava, A.; Thomas, D.; Lalor, P.; Dockery, P.; Pandit, A. Three-Dimensional Microgel Platform for the Production of Cell Factories Tailored for the Nucleus Pulposus. *Bioconjug. Chem.* **2014**, dx.doi.org/10.1021/bc5004247
- (36) Lee, J. Y.; Spicer, A. P. Hyaluronan: A Multifunctional, megaDalton, Stealth Molecule. *Curr. Opin. Cell Biol.* **2000**, *12*, 581–586.
- (37) Prehm, P. Hyaluronate Is Synthesized at Plasma Membranes. *J. Biomech.* **1984**, *220*, 597–600.
- (38) Prehm, P.; Schumacher, U. Inhibition of Hyaluronan Export from Human Fibroblasts by Inhibitors of Multidrug Resistance Transporters. *Biochem. Pharmacol.* **2004**, *68*, 1401–1410.
- (39) Shankar, H.; Scarlett, J. A.; Abram, S. E. Anatomy and Pathophysiology of Intervertebral Disc Disease. *Tech. Reg. Anesth. Pain Manag.* **2009**, *13*, 67–75.
- (40) Dougados, M.; Nguyen, M.; Listrat, V.; Amor, B. High Molecular Weight Sodium Hyaluronate (hyalectin) in Osteoarthritis of the Knee: A 1 Year Placebo-Controlled Trial. *Osteoarthritis Cartilage* **1993**, *1*, 97–103.
- (41) Karna, E.; Milyk, W.; Pałka, J. a; Jarzabek, K.; Wołczyński, S. Hyaluronic Acid Counteracts Interleukin-1-Induced Inhibition of Collagen Biosynthesis in Cultured Human Chondrocytes. *Pharmacol. Res.* **2006**, *54*, 275–281.
- (42) Savani, R. C.; Wang, C.; Yang, B.; Zhang, S.; Kinsella, M. G.; Wight, T. N.; Stem, R.; Nance, D. M.; Turley, E. A. Migration of Bovine Aortic Smooth Muscle Cells after Wounding Injury The Role of Hyaluronan and RHAMM. *J. Clin. Investig.* **1995**, *95*, 1158–1168.

- (43) Halloran, D. O.; Grad, S.; Stoddart, M.; Dockery, P.; Alini, M.; Pandit, A. S. An Injectable Cross-Linked Scaffold for Nucleus Pulposus Regeneration. *Biomaterials* **2008**, *29*, 438–447.
- (44) Jeffrey A., T.; Michael G., H.; James M., W.; William D., W.; Randolph L., G. Hyaluronan Enhances Contraction of Collagen by Smooth Muscle Cells and Adventitial Fibroblasts: Role of CD44 and Implications for Constrictive Remodeling. *Circ. Res.* **2001**, *88*, 77–83.
- (45) Ishida, O.; Tanaka, Y.; Morimoto, I.; Takigawa, M. Chondrocytes Are Regulated by Cellular Adhesion through CD44 and Hyaluronic Acid Pathway. *J. Bone Miner. Res.* **1997**, *12*, 1657–1663.
- (46) Day, A. J.; De La Motte, C. A. Hyaluronan Cross-Linking: A Protective Mechanism in Inflammation? *Trends Immunol.* **2005**, *26*, 637–643.
- (47) Huaping, T.; Alicia, D.; J. Peter, R.; Constance R., C.; Kacey G., M. Novel Multi-Arm PEG-Based Hydrogels for Tissue Engineering. *J. Biomed. Mater. Res. A* **2011**, *92*, 979–987.
- (48) Wieland, J. A.; Tiffany L. Houchin-Raya, and L. D. S. Non-Viral Vector Delivery from PEG-Hyaluronic Acid Hydrogels. *J. Control. Release* **2009**, *120*, 233–241.
- (49) Stern, R.; Asari, A. A; Sugahara, K. N. Hyaluronan Fragments: An Information-Rich System. *Eur. J. Cell Biol.* **2006**, *85*, 699–715.
- (50) Petrey, A. C.; De La Motte, C. A. Hyaluronan, a Crucial Regulator of Inflammation. *Front. Immunol.* **2014**, *5*, 101.
- (51) Hoyland, J. A; Le Maitre, C.; Freemont, A J. Investigation of the Role of IL-1 and TNF in Matrix Degradation in the Intervertebral Disc. *Rheumatology (Oxford)*. **2008**, *47*, 809–814.
- (52) Yung-Yang, L.; Cheng-Hung, L.; Rejmon, D.; Hang, Z.; Hicham, M.; Aviva, S.; Olga, S.; Pei-Ming, H.; Hari G., G.; Charles A., H.; Deborah A., Q. High-Molecular-Weight Hyaluronan- a Possible New Treatment for Sepsis-Induced Lung Injury: A Preclinical Study in Mechanically Ventilated Rats. *Crit. Care* **2008**, *12*, R102.
- (53) Forrester, J. V; Matrix, E. A. B. Inhibition of Phagocytosis by High Molecular Weight Hyaluronate. *J. Immunol.* **1980**, *40*, 435.
- (54) Schimizzi, A. L.; Massie, J. B.; Murphy, M.; Perry, A.; Kim, C. W.; Garfin, S. R.; Akeson, W. H. High-Molecular-Weight Hyaluronan Inhibits Macrophage Proliferation and Cytokine Release in the Early Wound of a Preclinical Postlaminectomy Rat Model. *Spine J.* **2006**, *6*, 550–556.

- (55) Aoki, Y.; Takahashi, Y.; Ohtori, S.; Moriya, H.; Takahashi, K. Distribution and Immunocytochemical Characterization of Dorsal Root Ganglion Neurons Innervating the Lumbar Intervertebral Disc in Rats: A Review. *Life Sci.* **2004**, *74*, 2627–2642.
- (56) Renn, C. L.; Leitch, C. C.; Dorsey, S. G. In Vivo Evidence That Truncated trkB.T1 Participates in Nociception. *Mol. Pain* **2009**, *5*, 61.
- (57) Barbara, Z.; Letizia, F.; Carlotta, G.; Girolamo, C.; Paola, B.; Roberta, C.; Giovanni, A.; Paolo, P. Hyaluronic Acid Induces Activation of the K-Opioid Receptor. *PLoS One* **2013**, *8*, 1–8.
- (58) Ponta, H.; Sherman, L.; Herrlich, P. A. CD44: From Adhesion Molecules to Signalling Regulators. *Nat. Rev. Mol. Cell Biol.* **2003**, *4*, 33–45.
- (59) Svee, K.; White, J.; Vaillant, P.; Jessurun, J.; Roongta, U.; Krumwiede, M.; Johnson, D.; Henke, C. Acute Lung Injury Fibroblast Migration and Invasion of a Fibrin Matrix Is Mediated by CD44. *J. Clin. Invest.* **1996**, *98*, 1713–1727.
- (60) Carol A., de la M.; Vincent C., H.; Judith, D.; Sudip K., B.; Scott A., S. Mononuclear Leukocytes Bind to Specific Hyaluronan Structures on Colon Mucosal Smooth Muscle Cells Treated with Polyinosinic Acid: Polycytidylic Acid. *Am. J. Pathol.* **2003**, *163*, 121–133.

## Table of Contents

